Published in final edited form as:
J Neurosurg. 2014 March ; 120(3): 628–638. doi:10.3171/2013.10.JNS13918.

Overexpression of adenosine kinase in cortical astrocytes generates focal neocortical epilepsy in mice: Laboratory investigation

Hai-Ying Shen, M.D., Ph.D.[1,*], **Hai Sun, M.D., Ph.D.**[2,*], **Marissa M. Hanthorn, B.A.**[1], **Zhongwei Zhi, B.S.**[3], **Jing-Quan Lan, M.D.**[1], **David J. Poulsen, M.Sc., Ph.D.**[4], **Ruikang K. Wang, M.Sc., Ph.D.**[3], and **Detlev Boison, Ph.D**[1,#]

[1]Robert Stone Dow Neurobiology Laboratories, Legacy Research Institute, Portland, OR

[2]Department of Neurological Surgery, Oregon Health & Science University, Portland, OR

[3]Department of Bioengineering, University of Washington, Box 355061, Seattle, WA

[4]Department of Biomedical and Pharmaceutical Sciences, University of Montana, Missoula, MT

Abstract

Object—New experimental models and diagnostic methods are needed to better understand the pathophysiology of focal neocortical epilepsies in a search for improved epilepsy treatment options. We hypothesized that a focal disruption of adenosine homeostasis in the neocortex might be sufficient to trigger electrographic seizures. We further hypothesized that a focal disruption of adenosine homeostasis might affect microcirculation and thus offer a diagnostic opportunity for the detection of a seizure focus located in the neocortex.

Methods—Focal disruption of adenosine homeostasis was achieved by injecting an adeno-associated virus (AAV) engineered to overexpress adenosine kinase (ADK), the major metabolic clearance enzyme for the brain's endogenous anticonvulsant adenosine, into the neocortex of mice. Eight weeks following virus injection, the affected brain area was imaged via optical microangiography (OMAG) to detect changes in microcirculation. After completion of imaging, cortical electroencephalography (EEG) recordings were obtained from the imaged brain area.

Results—Viral expression of the *Adk* cDNA in astrocytes generated a focal area (~ 2 mm in diameter) of ADK overexpression within the neocortex. OMAG scanning revealed a reduction in vessel density within the affected brain area of approximately 23% and 29% compared to control animals and the contralateral hemisphere, respectively. EEG recordings revealed electrographic seizures within the focal area of ADK overexpression at a rate of 1.3 ± 0.2 seizures per hour.

Conclusions—Our findings suggest that focal adenosine deficiency is sufficient to generate a neocortical focus of hyperexcitability, which is also characterized by reduced vessel density. We conclude that our model constitutes a useful tool to study neocortical epilepsies and that OMAG constitutes a non-invasive diagnostic tool for the imaging of seizure foci with disrupted adenosine homeostasis.

[#]Corresponding author Detlev Boison, Ph.D., RS Dow Neurobiology Laboratories, Legacy Research Institute, 1225 NE 2nd Avenue, Portland OR 97232, Tel: (503)413-1754, Fax: (503)413-5465, dboison@downeurobiology.org.
[*]Equal contributing authors

Disclosure
Dr. Sun is in receipt of funds from the Congress of Neurological Surgeons Christopher C. Getch Flagship Fellowship Award. A portion of this work was presented at the 80th Annual Scientific meeting of the American Association of Neurological Surgeons and was featured in the meeting press release. None of the authors has any conflicts of interest to disclose.

Keywords

adenosine kinase; adeno-associated virus; neocortical epilepsy; optical microangiography; mice

Disruption of adenosine homeostasis is a pathological hallmark of temporal lobe epilepsy and therapeutic adenosine augmentation is a rational approach for seizure control.[5–7] Adenosine homeostasis in the brain is largely under the control of adenosine kinase (ADK); the key metabolic clearance enzyme for adenosine.[2] In the adult brain ADK is predominantly expressed in astrocytes,[59] where the expression levels of the enzyme determine the extent of a transmembrane gradient for adenosine, which under baseline conditions, drives the influx of adenosine into the astrocyte through equilibrative nucleoside transporters.[7,9,15,19] Therefore, synaptic levels of adenosine are largely under the control of astrocytes, which form a sink for the metabolic clearance of adenosine.[9,15,17] We have previously demonstrated that astrogliosis and associated pathological overexpression of ADK is linked to neuronal hyperexcitability and seizure activity in rodent models of temporal lobe epilepsy (TLE),[3,40] whereas surgically resected specimens from human patients with TLE were likewise characterized by profound overexpression of ADK.[3,43] Conversely, genetic or virus-induced reduction of ADK expression in the hippocampus was shown to suppress seizures,[40,60] while focal cell-based adenosine augmentation to the hippocampus was shown to protect the hippocampal formation from injury and seizures.[40,41] Together, these findings demonstrate that adenosine homeostasis, controlled by astrocytic ADK, critically determines excitability of the hippocampus. However, whether this is true for other brain regions and other forms of epilepsy has not been investigated.

In addition to its direct control of neuronal function, adenosine signaling regulates vascular functions, which may contribute to the brain's susceptibility to seizures.[1,47,50,51] Acutely, adenosine promotes hemodynamic events, such as vasodilation to increase blood flow in the brain, in response to hypoxia or ischemia.[12,50,51] Adenosine, largely derived from the breakdown of ATP during conditions of energetic crisis, cell swelling, and acidosis, affects cerebral blood flow mostly via activation of adenosine A_{2A} receptors in balancing blood flow with metabolism. The primary effect of A_{2A} receptors stimulation is activation of K_{ATP} and K_{Ca} channels resulting in smooth muscle relaxation and elevated blood flow rates.[50] Further it has been shown that inhibition of ADK increases cerebral blood flow (CBF) by augmenting interstitial adenosine levels.[56] In addition, chronically increased levels of adenosine have been shown to stimulate angiogenesis[1,29,49] Consequently, chronic overexpression of ADK, as seen in epilepsy, may result in reduced CBF and reduction of local vasculature. Therefore, ADK-dependent changes in vasculature might provide a diagnostic opportunity for the detection of an epileptogenic focus that is characterized by overexpression of ADK.

This study was designed to assess whether overexpression of ADK links to neuronal hyperexcitability and seizure activity in the neocortex, as well as to develop a diagnostic method to identify cortical areas of neuronal hyperexcitability. Compared to TLE, the pathophysiology and mechanisms for seizure generation in neocortical epilepsy (NCE) are understudied. In particular, a scarcity of clinically relevant rodent models for NCE has limited research progress.[33,45,48] In addition, NCE remains one of the most difficult to treat forms of epilepsy and improved diagnostic methods, which account for pathophysiological mechanisms of NCE, need to be developed.[20,54,66]

Since astroglial ADK regulates neuronal excitability of the hippocampus as well as microcirculation, we hypothesized that a focal disruption of adenosine homeostasis induced by overexpressing ADK in astrocytes in the neocortex might be sufficient to induce neuronal

hyperexcitability and changes in microcirculation. We used adeno-associated virus 8 (AAV8)-based viral vectors to overexpress ADK in astrocytes of the neocortex.[57] To demonstrate ADK-related changes in microcirculation we used a novel imaging technology, optical microangiography (OMAG),[30–32] which is based on endogenous light scattering from biological tissue. This non-invasive technology allows generation of microstructural and functional vascular images that can resolve the 3D distribution of dynamic blood perfusion at the capillary level resolution *in vivo*.[30–32] Here, we evaluated OMAG as a potential diagnostic tool to detect focal microcirculation changes in the vicinity of focal areas with disrupted adenosine homeostasis. Our data demonstrate that focal overexpression of ADK in astrocytes of the neocortex is sufficient to elicit electrographic seizures with concomitant changes in microcirculation. Our findings are of significance to understand mechanisms of seizure generation in NCE and demonstrate the diagnostic value of the non-invasive OMAG approach to identify focal neocortical areas of hyperexcitability.

Methods

Animals

All animal procedures were performed in an Association for the Assessment and Accreditation of Laboratory Animal Care-accredited facility in accordance with protocols approved by the Institutional Animal Care and Use Committees of the Legacy Research Institute and the Oregon Health & Science University, and the principles outlined in the National Institutes for Health guide for the Care and Use of Laboratory Animals. C57BL/6 male mice (20–30 g) were subjected to neocortical virus injection followed by OMAG and EEG (Fig. 1A). All animals were group-housed with water and food available ad libitum in temperature- and humidity-controlled rooms with a 12-h light/dark cycle throughout the experimental period.

Adeno-associated virus production and delivery

As described previously [57,60] the short cytoplasmic isoform of ADK was introduced into an adeno-associated virus (AAV) based system in which ADK cDNA was placed under the control of the astrocyte-specific gfaABC1D promoter.[37] This vector is designated as ADK-SS. An AAV8-pGfa-null (AAV-Null) virus containing an empty vector backbone was used as a negative control vector. Virus production and titer determination was performed as described previously.[57,60] For virus delivery, the ADK-SS or AAV-Null virus was unilaterally injected into the right side of the neocortex under general anesthesia (1.5% isoflurane, 70% N_2O and 28.5% O_2), in a volume of 0.5 μl of concentrated viral solution (10^{12} genomic particles/ml), with stereotactic coordinates (anteroposterior (AP)=−2.10 mm; mediolateral (ML)=−1.50 mm; dorsoventral (DV)=−0.80 mm). After the cortical injections, all animals were sutured, disinfected, and then returned to the home cage.

Optical microangiography

To test whether focal disruption of adenosine homeostasis affects cortical microcirculation, CBF was measured in mice 8 weeks after viral delivery, using OMAG; a high-resolution optical coherence tomography technique that is capable of producing 3-D images of dynamic blood perfusion within microcirculatory tissue beds at an imaging depth up to 2 mm below the surface.[31] For example, OMAG is able to measure changes of cerebral blood perfusion in response to systemic hypoxia and hyperoxia.[31] Since OMAG requires intact cerebral cortex, this step was performed before the EEG recordings (Fig. 1A). Prior to imaging, the mouse was immobilized in a custom made stereotaxic stage under general anesthesia (1.5% isoflurane, 70% N_2O and 28.5% O_2) and the mouse head was shaved and depilated. The body temperature was maintained between 35.5°C to 36.5°C with a thermostat-controlled heating pad (Harvard Apparatus, MA). An incision of 1 cm was made

along the sagittal suture, and the frontal parietal and interparietal bones were exposed by pulling the skin to the sides. The animal was then positioned under the OMAG scanning probe. In order to acquire microvascular images over a large area of the cortex, scanning was performed clockwise, which resulted in six to eight OMAG images per mouse covering both hemispheres over an area of approximately 4x5 mm (Fig. 1B). The total imaging time per mouse was less than 10 minutes. After imaging and data acquisition, blood flow signals were isolated from each 3-D OMAG data set using a volume segmentation algorithm.[61–63] The volume segmentation algorithm was applied to each OMAG data set to isolate blood flow signals within the cortex. A maximum projection method was then used to project the blood flow signals into the x-y plane to reduce the image size. The final OMAG image, including the area of the viral injection site and the corresponding area in the contralateral hemisphere, was obtained by assembling six (or eight if necessary) individual images. The cerebral blood perfusion was estimated by computing the functional vessel density in the area of interest in the final OMAG image.[53] To achieve this, the OMAG image was first converted to a binary flow map by setting a fixed intensity threshold. A circular area with diameter of 2 mm centered at the viral injection site was identified on the flow map. The percentage of pixels with binary value of 1s versus pixel numbers of the whole area was calculated as the estimation of vessel density, i.e., the quantitative equivalence of cerebral blood perfusion.[53] The cerebral blood perfusion in the corresponding area in the contralateral hemisphere was estimated using the same method. Statistical comparisons of vessel density between the ADK-SS virus-injected animals and the control animals (injected with AAV-null virus) were then undertaken. Additional comparisons were made with the virus-injected sites and their corresponding contralateral locations. The processing and analysis on the OMAG images was carried out using MATLAB programing software (Natick, MA).

Electroencephalography

Three days following the OMAG scan bipolar, coated stainless steel electrodes (80 μm in diameter; Plastics One) were implanted into the virus-injected cortex (coordinates: AP=−2.1 mm; ML=−1.5 mm; DV=−1.0 mm with bregma as reference) under general anesthesia. A cortical screw electrode (AP=1.0 mm, ML=1.5 mm) and a ground reference electrode (AP=6.0 mm; ML=0 mm) were placed over the frontal cortex and cerebellum, respectively (Fig. 1B). All electrodes were secured to the skull with dental cement. One week later, EEG monitoring was performed as previously described[60] with modifications as follows. After habituation to the EEG-recording procedure for 4 hours, mice were recorded by EEG for an additional 24 hours. Quantification of the EEG data was performed by an investigator who was blinded to the experimental treatment. An electrographic seizure was defined as high-amplitude rhythmic discharge that clearly represented a new pattern of tracing lasting for > 5 sec (repetitive spikes, spike-and-wave discharges, or slow waves). Epileptic events occurring with an interval < 5 sec without the EEG returning to baseline were defined as belonging to the same seizure. Seizures were primarily electrographic in nature, but frequently accompanied by arrest or staring episodes, however, no concurrent convulsions were observed. Seizure quantification was processed exclusively by intracortical EEG recordings.

Immunohistochemistry

To determine changes in ADK expression, virus-injected mice were sacrificed after EEG evaluation for immunohistochemical analysis as previously described.[59] For the detection of ADK, a primary anti-ADK antibody (1:5000)[59] was used. To detect the cell-type specificity of ADK expression,[57] double immunofluorescence staining was performed using a combination of primary antibodies directed against ADK (polyclonal, rabbit) and glial fibrillary acidic protein (GFAP; monoclonal, mouse 1:400, MAB360, Chemicon

International, CA), or NeuN (Neuronal Nuclei; monoclonal, mouse 1:750, MAB377, Chemicon). Nissl staining was performed separately on adjacent brain slices. Digital images were acquired using a Zeiss AxioPlan inverted microscope equipped with an AxioCam 1Cc1 camera (Carl Zeiss MicroImaging, Thornwood, NY). To quantitatively evaluate the expression level of ADK, the optical density (OD) of ADK positive staining was measured using Image-Pro Plus software (version 5.1, Media Cybernetics, Inc., Silver Spring, MD) as described[40] using two coronal brain sections at the level of the virus-injection from each animal. Data were normalized to the contralateral cortical ADK expression levels.

Statistical analysis

Data are expressed as means ± standard error of mean (SEM). Statistical analysis was performed by a one way analysis of variance (ANOVA) followed by Bonferroni post-hoc analysis or student t-test. $P < 0.05$ was considered statistically significant.

Results

Focal overexpression of ADK in astrocytes within the neocortex

To determine changes in ADK expression, 8 weeks following virus injection and after completion of OMAG imaging and EEG-recordings (Fig. 1A), animals were sacrificed and brains evaluated histologically. Nissl staining to assess general brain morphology did not reveal any gross morphological deviations in virus-injected animals compared to control; in particular, virus-injection was not associated with any overt signs of pyknosis, karyolysis or shrunken cell bodies (Fig. 1C, lower panel). The lack of any obvious virus-induced cytotoxic effects is in line with the demonstrated safety-profile of the AAV system for CNS applications.[64,65] Immunohistochemistry data demonstrated that the cortical injection of the ADK-SS virus induced a focal overexpression of ADK within the injected neocortex (Fig. 1C), whereas injection of the AAV-Null virus had no obvious effects on ADK expression patterns, which were comparable to the non-injected contralateral cortex (Fig. 1C). Quantitative analysis of immunodensities demonstrated that the ADK-SS virus induced a robust focal increase in ADK expression, which showed a 4.8 ± 0.86-fold increase compared to ADK expression levels in the contralateral hemisphere ($p<0.01$, n=5 per group) and a 4.4 ± 0.77-fold increase compared to the AAV-Null injected hemisphere ($p<0.01$, n=5 per group) (Fig. 1C). Conversely, AAV-Null virus injection did not cause significant changes in ADK expression compared to the contralateral hemisphere ($p>0.05$, n=5 per group) (Fig. 1C). We previously demonstrated in a transgenic model system that a 63.6% increase in ADK resulted in a 50% reduction in the ambient tone of adenosine;{Shen, 2011 #8692 we therefore conclude that the focal overexpression of ADK achieved here triggers a local deficiency in adenosine. To identify the rostral caudal extent of ADK-SS induced ADK overexpression a series of brain slices was investigated spanning from −1.70 to −2.75 mm from bregma (Fig. 1D). Analysis of the extent of virus-induced ADK overexpression demonstrated a focal area of high levels of ADK within the neocortex with a diameter about 1.9 ± 0.4 mm (n=5).

Higher resolution images of ADK immunoperoxidase stained sections demonstrated profound differences in the subcellular localization of ADK between experimental groups (Fig. 2A). Images from ADK-SS injected cortex showed high levels of ADK expression in cell somata and cellular processes, consistent with overexpression of the cytoplasmic isoform of ADK as expressed by the virus. ADK-positive cells had characteristic morphological features of astrocytes, with a star-like appearance and several primary processes originating from the soma (Fig. 2A, inset). In contrast ADK expression in control samples from AAV-Null animals had a characteristic pattern of prominent nuclear ADK expression coupled with a diffuse homogenous staining of ADK throughout the tissue at

much lower levels in line with our previous characterization of astrocytic ADK expression in naïve mice.{Gouder, 2004 #2910; Studer, 2006 #7880} To confirm the cell-type specificity of ADK-SS-induced ADK overexpression a double immunofluorescence analysis was performed by co-staining ADK with either GFAP or NeuN (Fig. 2B and 2C). As expected, and in line with our previous work,[57,60] ADK expression was colocalized with and confined to GFAP-positive cells (Fig. 2B, left panel) but not NeuN-positive cells (Fig. 2B, right panel). Higher resolution images confirmed the differential expression pattern of ADK-SS induced overexpression of exogenous ADK (cytoplasm) versus endogenous ADK (nucleus) (Fig. 2C). Together, our data demonstrate a robust focal overexpression of the cytoplasmic isoform of ADK in cortical astrocytes from ADK-SS injected mice. Importantly, overexpression of ADK was confined to a distinct focal area with a diameter of about 2 mm close to the cortical surface, whereas other brain areas were not affected by ADK-SS or a control virus injection.

Focal overexpression of ADK in astrocytes triggered recurrent electrographic seizures in the neocortex

To evaluate whether focal neocortical overexpression of ADK influenced neuronal excitability, we performed continuous EEG monitoring of neocortical electrographic activity, 8 to 9 weeks after intracortical injection of ADK-SS or AAV-Null virus. EEG recordings from the neocortical injection site illustrated that ADK-SS virus-injected mice developed spontaneous recurrent electrographic seizures within the neocortex (Fig. 3A, lower panel) whereas AAV-Null virus injected animals were devoid of any seizure activity (Fig. 3A, upper panel). The neocortical electrographic seizures were characterized by a gradual increase in amplitude that became rhythmic at the beginning of the seizure (Fig. 3A, lower panel, closed arrow) whereas the end of the seizure had an overt drop in amplitude (Fig. 3C, lower panel, open arrow). The neocortical seizures, which occurred in the ADK-SS injected animals had a seizure frequency of 1.3 ± 0.2/hour ($n = 8$) with an average duration of 94 ± 8 s. It is important to note that even though spontaneous electrographic seizures were observed in all animals with ADK overexpression those activities were not associated with any convulsive behavior. Power spectral analysis of the single event depicted in Fig. 3A indicates a predominant ictal frequency of around 3 Hz (Fig. 3C), which is in contrast to interictal EEG activity from ADK-SS recipients or baseline activity in AAV-Null recipients (Fig. 3B). Together, the EEG data demonstrated that focal viral overexpression of ADK within astrocytes was sufficient to trigger spontaneous recurrent neocortical seizures in the absence of any epileptogenic event.

Reduced focal vessel density in ADK-SS injected mice

To evaluate whether disruption of adenosine homeostasis causes changes in microcirculation, we employed the OMAG approach to image dynamic *in vivo* cerebral blood perfusion and vasculature changes on the mice 8 weeks after viral injection. The high contrast OMAG images demonstrated well-resolved cerebral vasculature indicating the CBF status of the mice (Fig. 4A). OMAG data showed that the AAV-Null virus injection did not cause focal changes in cerebral blood perfusion and vessel density similar to the contralateral hemisphere (Fig. 4A, left panel). Importantly, OMAG images showed that ADK-SS induced overexpression of ADK resulted in an overt reduced local cerebral vessel density indicating reduced cerebral blood perfusion, surrounding the viral injection site (Fig. 4A, right panel). The resulting quantitative data demonstrated a significant reduction of focal cerebral blood perfusion in the ipsilateral neocortex of ADK-SS recipients compared to the corresponding region in AAV-Null recipients (23 % reduction of CBF, $P<0.05$, $n=5$, Fig. 4B, left panel). Likewise, the focal vessel density in the ipsilateral neocortex of ADK-SS was also significantly lower (29 % reduction) compared to the contralateral hemisphere of the same animal (29% reduction of vessel density, $P<0.05$, $n=5$, Fig. 4B, right panel).

Together, the analysis of the OMAG data indicated that disruption of adenosine homeostasis by overexpression of ADK led to a reduction in focal cerebral blood perfusion and cerebral vessel density.

Discussion

To better understand mechanisms of ictogenesis in NCE, we report here a novel animal model of NCE with neocortical overexpression of ADK in astrocytes, and demonstrate the feasibility of OMAG as an advanced non-invasive imaging tool to detect the epileptic focus in this model. We demonstrate the following key findings: *(i)* virus-induced overexpression of astrocytic ADK in neocortex is sufficient to produce robust spontaneous recurrent focal electrographic seizures at a frequency of 1.3 ± 0.2 seizures per hour, and *(ii)* the seizure generating focus spatially aligns with overexpression of ADK and detectable microcirculation changes, which can be evaluated non-invasively by OMAG. [4729,49–51156] ADK is the key enzyme for the metabolic clearance of adenosine and exists in two isoforms, which are specific for the nucleus (ADK long; ADK-L) or the cytoplasm (ADK short, ADK-S).[8] The specific roles of the different isoforms have not yet been fully elucidated, but mounting evidence suggests that nuclear ADK-L plays a role in epigenetic functions and cell proliferation, whereas the cytoplasmic ADK-S appears to be responsible for the metabolic clearance of extracellular adenosine.[8]

As our current findings validate (Fig. 2A), and as previously demonstrated,[22,59] under control or baseline conditions, the majority of ADK expression is confined to the nucleus or perinuclear area of astrocytes. However, in the epileptic brain astrocytic ADK is not only increased in quantity, but also in subcellular distribution with a robust shift of ADK expression from the perinuclear area into the network of astrocyte processes.[40] Therefore, quantity and distribution of the cytoplasmic isoform of ADK might play a key role in ictogenesis. We therefore overexpressed the cytoplasmic isoform of ADK in astrocyte and show profound expression of ADK in astrocytic processes (Fig. 2C) similar to ADK expression patterns in a mouse model of kainic acid induced epilepsy.[40] Our demonstration that overexpression of the cytoplasmic isoform of ADK in astrocytes is sufficient to trigger focal neocortical seizures, further supports a role of ADK located in astrocyte processes for ictogenesis.

While AAV-induced overexpression of ADK within astrocytes was sufficient to trigger spontaneous electrographic seizures in the neocortex, none of the subjects in this study exhibited any signs of convulsive seizures. Periods of immobility or staring episodes were occasionally associated with the electrographic seizures indicating a phenotype of partial epilepsy without generalization. The hourly seizure rate, as well as the brief duration (94 seconds) of the seizures and the low intra-ictal spike frequency (3Hz), is in line with electrographic seizure patterns that have been linked to deficient adenosine signaling. Focal CA3 selective seizures (4.3 seizures per h; 17.5 sec duration), linked to astrogliosis and overexpression of ADK after intraamygdaloid kainic acid injection, spontaneous seizures in Adk-tg mice with brain-wide overexpression of ADK (4.8 seizures per hour; 26.7 sec duration), and spontaneous seizures in adenosine A_1R knockout mice (5.3 seizures per hour; 27.8 sec duration) all share the same characteristic seizure pattern with an intra-ictal spike frequency of 3–4 Hz.[38] Together these findings suggest that overexpression of ADK, resulting in deficient signaling through the A_1R, triggers a characteristic seizure pattern also found in focal seizure models that result from a precipitating status epilepticus. Since ADK expression was found to be focally restricted to a sphere with a diameter of about 2 mm (Fig. 1), adenosine homeostasis in the remaining brain is not likely to be compromised by this manipulation. The lack of seizure spread in this model is consistent with previous findings demonstrating that adenosine A_1R activation by endogenous adenosine is a

prerequisite for the prevention of seizure spread.[18,39] Thus, a local deficiency of adenosine caused by the cell-type selective overexpression of ADK in astrocytes, triggers focal electrographic seizures by insufficient activation of the A_1R, which normally limits neuronal excitability by mediating presynaptic inhibition and by stabilizing the postsynaptic membrane potential. The focal nature of our manipulation is further supported by OMAG imaging suggesting a tight spatial match between overexpression of ADK and changes in the microvasculature.

Adenosine is one of the most potent vasodilators in different kinds of tissues and organs. Under both physiological and pathophysiological conditions extracellular adenosine provokes acute local vasodilation within the cerebral microcirculature[47] mainly via activation of the cAMP pathway through adenosine A_{2A} and A_{2B} receptors.[49–51] Studies also suggest that adenosine exerts long-term effects on microvasculature via facilitation of angiogenesis[1] through the induction of angiogenic growth factors such as vascular endothelial growth factor.[1] Whereas the application of adenosine or pharmacological agents that alter adenosine metabolism can stimulate vasodilation and blood vessel growth, the inhibition of ADK can increase CBF through an increase in interstitial adenosine levels.[56]

While not directly investigated here due to space considerations, we have demonstrated previously that the overexpression of astrocytic ADK leads to a robust reduction in ambient adenosine levels[15,57], whereas downregulation of endogenous ADK is a physiological response to raise adenosine levels under conditions of metabolic or energetic stress.[52] The reduced vessel density and reduced cerebral blood perfusion demonstrated here (Fig. 4) are consistent with a reduced concentration of adenosine in the neocortical focus of overexpressed ADK and reduced activation of the vascular $A_{2A}R$, which plays an important role in the regulation of CBF and angiogenesis.[50]. Given the lower sensitivity of the $A_{2A}R$ compared to the A_1R even a minor reduction in adenosine is likely to affect the vasculature. In addition, seizures by themselves are known to trigger the release of adenosine as an endogenous mechanism contributing to seizure termination[16,35] and seizure-induced adenosine release is consistent with an increase of CBF during ictal seizure events.[21,34] Our findings of consistently reduced CBF within the ADK-related seizure focus suggest that seizure-induced elevations of adenosine are subject to enhanced metabolic clearance through increased levels of ADK and therefore no longer effective in influencing CBF. Astrocytes play a central role in the vasomotor response, in which neurovascular coupling links massive Ca^{2+} elevations in the ictal phase to changes in CBF.[21] However, a reduced basal adenosine level may lead to a loss of postictal cerebral vasodilation.[14,47] Given the frequent occurrence and long duration of ADK-induced neocortical eletrographic seizures, it is likely that the net effects of the CBF measurement obtained by OMAG are based on a combination of ictal and interictal events.

Clinically, neocortical epileptogenic brain areas may surgically be resected following presurgical evaluation through a variety of techniques:[20] *(i)* computerized EEG source imaging, based on surface or invasive intracranial EEG, targets focal abnormal epileptic activity;[44] *(ii)* neuroimaging approaches, such as positron emission tomography, single photon emission computed tomography, or functional magnetic resonance imaging are used to detect regional cerebral blood volumes;[27,28,46] and *(iii)* computerized tomography (CT) and magnetic resonance (MR) imaging are used to detect epilepsy-related dysplasias.[10] However, each of the above approaches has its own set of limitations in diagnostic sensitivity and predictive value.[36] Alternative or additional diagnostic approaches might be useful to improve planning of a surgical resection[4,58] and are in particular need for neocortical epilepsy, since this condition in general shows a lower rate of concordance between diagnostic modalities as compared to mesial TLE.[36] Changes in neuronal activities are known to alter the light scattering and absorption properties of brain tissue. The intrisinc

optical signal imaging technique provides 2D cortical maps of these changes and has been used to study the functional organization of visual cortex[23,42] and to perform intraoperative mapping of functional and epileptiform activities in human subjects.[11,24–26,55] These 2D techniques are only able to detect hemodynamic changes on the cortical surface with limited spatial resolution. The novel imaging technology OMAG investigated here is based on endogenous light scattering from biological tissue to obtain microstructural and functional vascular images, and can resolve the 3D distribution of dynamic blood perfusion at capillary level resolution within the microcirculatory bed *in vivo*.[31] In the present study, we demonstrate that OMAG is able to detect a region with changes of microvasculature and blood perfusion in a diameter of 2 mm, which reflects the area with overexpression of virus-induced ADK. This finding indicates that a potentially small neocortical epileptic focus might be detectable with OMAG, a technology that is non-invasive and reproducibly delivers high resolution (100 μm) images without the need of exogenous contrasting agents, as usually needed for CT, MR imaging or positron emission tomography.[63] We show here that OMAG can reliably be used as a diagnostic tool to detect focal overexpression of ADK. Since overexpression of ADK appears to be a common pathological hallmark found in many different forms of experimental and clinical epilepsy,[2,3,13,22,39,40,43] OMAG presents as a novel diagnostic tool to identify focal areas of increased ADK expression as predictors for epileptogenic zones.

Acknowledgments

The authors thank Hrebesh M. Subhash and Brian Anderson for their technical support and Shirley McCartney, PhD, for editorial assistance.

This work was supported by grant R01 NS061844 (DB) from the National Institutes of Health.

References

1. Adair TH. Growth regulation of the vascular system: an emerging role for adenosine. Am J Physiol Regul Integr Comp Physiol. 2005; 289:R283–R296. [PubMed: 16014444]
2. Aronica E, Sandau US, Iyer A, et al. Glial Adenosine Kinase – a Neuropathological Marker of the Epileptic Brain. Neurochem Int. 2013 in press.
3. Aronica E, Zurolo E, Iyer A, et al. Upregulation of adenosine kinase in astrocytes in experimental and human temporal lobe epilepsy. Epilepsia. 2011; 52:1645–1655. [PubMed: 21635241]
4. Blume WT, Ganapathy GR, Munoz D, et al. Indices of resective surgery effectiveness for intractable nonlesional focal epilepsy. Epilepsia. 2004; 45:46–53. [PubMed: 14692907]
5. Boison D. Adenosine augmentation therapies (AATs) for epilepsy: prospect of cell and gene therapies. Epilepsy Res. 2009; 85:131–141. [PubMed: 19428218]
6. Boison, D. Adenosine augmentation therapy for epilepsy. In: Noebels, JL.; Avoli, M.; Rogawski, MA., et al., editors. Jasper's Basic Mechanisms of the Epilepsies. 4. Oxford: Oxford University Press; 2012. p. 1150-1160.
7. Boison D. Adenosine dysfunction in epilepsy. Glia. 2012; 60:1234–1243. [PubMed: 22700220]
8. Boison D. Adenosine kinase: exploitation for therapeutic gain. Pharmacological Reviews. 2013; 65:906–943. [PubMed: 23592612]
9. Boison D, Chen JF, Fredholm BB. Adenosine signalling and function in glial cells. Cell Death Differ. 2010; 17:1071–1082. [PubMed: 19763139]
10. Bulakbasi N, Bozlar U, Karademir I, et al. CT and MRI in the evaluation of craniospinal involvement with polyostotic fibrous dysplasia in McCune-Albright syndrome. Diagn Interv Radiol. 2008; 14:177–181. [PubMed: 19061160]
11. Cannestra AF, Pouratian N, Bookheimer SY, et al. Temporal spatial differences observed by functional MRI and human intraoperative optical imaging. Cereb Cortex. 2001; 11:773–782. [PubMed: 11459767]

12. Coney AM, Marshall JM. Contribution of adenosine to the depression of sympathetically evoked vasoconstriction induced by systemic hypoxia in the rat. J Physiol. 2003; 549:613–623. [PubMed: 12702736]
13. de Groot M, Iyer A, Zurolo E, et al. Overexpression of ADK in human astrocytic tumors and peritumoral tissue is related to tumor-associated epilepsy. Epilepsia. 2012; 53:58–66. [PubMed: 22092111]
14. DiGeronimo RJ, Gegg CA, Zuckerman SL. Adenosine depletion alters postictal hypoxic cerebral vasodilation in the newborn pig. Am J Physiol. 1998; 274:H1495–1501. [PubMed: 9612355]
15. Diógenes MJ, Neves-Tomé R, Fucile S, et al. Homeostatic control of synaptic activity by endogenous adenosine is mediated by adenosine kinase. Cerebral Cortex. 2012 in press.
16. During MJ, Spencer DD. Adenosine: a potential mediator of seizure arrest and postictal refractoriness. Ann Neurol. 1992; 32:618–624. [PubMed: 1449242]
17. Etherington LA, Patterson GE, Meechan L, et al. Astrocytic adenosine kinase regulates basal synaptic adenosine levels and seizure activity but not activity-dependent adenosine release in the hippocampus. Neuropharmacology. 2009; 56:429–437. [PubMed: 18957298]
18. Fedele DE, Li T, Lan JQ, et al. Adenosine A_1 receptors are crucial in keeping an epileptic focus localized. Exp Neurol. 2006; 200:184–190. [PubMed: 16750195]
19. Fredholm BB. Rethinking the purinergic neuron-glia connection. Proc Natl Acad Sci U S A. 2012; 109:5913–5914. [PubMed: 22509008]
20. Gelziniene G, Endziniene M, Vaiciene N, et al. Presurgical evaluation of epilepsy patients. Medicina (Kaunas). 2008; 44:585–592. [PubMed: 18791335]
21. Gomez-Gonzalo M, Losi G, Brondi M, et al. Ictal but not interictal epileptic discharges activate astrocyte endfeet and elicit cerebral arteriole responses. Front Cell Neurosci. 2011; 5:8. [PubMed: 21747758]
22. Gouder N, Scheurer L, Fritschy J-M, et al. Overexpression of adenosine kinase in epileptic hippocampus contributes to epileptogenesis. J Neurosci. 2004; 24:692–701. [PubMed: 14736855]
23. Grinvald A. Optical imaging of architecture and function in the living brain sheds new light on cortical mechanisms underlying visual perception. Brain Topogr. 1992; 5:71–75. [PubMed: 1489652]
24. Haglund MM, Hochman DW. Furosemide and mannitol suppression of epileptic activity in the human brain. J Neurophysiol. 2005; 94:907–918. [PubMed: 15728766]
25. Haglund MM, Hochman DW. Optical imaging of epileptiform activity in human neocortex. Epilepsia. 2004; 45 (Suppl 4):43–47. [PubMed: 15281958]
26. Haglund MM, Ojemann GA, Hochman DW. Optical imaging of epileptiform and functional activity in human cerebral cortex. Nature. 1992; 358:668–671. [PubMed: 1495561]
27. Haughton V, Biswal B. Clinical application of basal regional cerebral blood flow fluctuation measurements by FMRI. Adv Exp Med Biol. 1998; 454:583–590. [PubMed: 9889938]
28. Henry TR. PET: cerebral blood flow and glucose metabolism--presurgical localization. Adv Neurol. 2000; 83:105–120. [PubMed: 10999192]
29. Hong KW, Shin HK, Kim HH, et al. Metabolism of cAMP to adenosine: role in vasodilation of rat pial artery in response to hypotension. Am J Physiol. 1999; 276:H376–382. [PubMed: 9950836]
30. Jia Y, Li P, Dziennis S, et al. Responses of peripheral blood flow to acute hypoxia and hyperoxia as measured by optical microangiography. PLoS One. 2011; 6:e26802. [PubMed: 22046363]
31. Jia Y, Li P, Wang RK. Optical microangiography provides an ability to monitor responses of cerebral microcirculation to hypoxia and hyperoxia in mice. J Biomed Opt. 2011; 16:096019. [PubMed: 21950933]
32. Jia Y, Qin J, Zhi Z, et al. Ultrahigh sensitive optical microangiography reveals depth-resolved microcirculation and its longitudinal response to prolonged ischemic event within skeletal muscles in mice. J Biomed Opt. 2011; 16:086004. [PubMed: 21895316]
33. Kondo S, Najm I, Kunieda T, et al. Electroencephalographic characterization of an adult rat model of radiation-induced cortical dysplasia. Epilepsia. 2001; 42:1221–1227. [PubMed: 11737155]

34. Kuhl DE, Engel J Jr, Phelps ME, et al. Epileptic patterns of local cerebral metabolism and perfusion in humans determined by emission computed tomography of 18FDG and 13NH3. Ann Neurol. 1980; 8:348–360. [PubMed: 6776878]
35. Lado FA, Moshe SL. How do seizures stop? Epilepsia. 2008; 49:1651–1664. [PubMed: 18503563]
36. Lee SK, Lee SY, Kim KK, et al. Surgical outcome and prognostic factors of cryptogenic neocortical epilepsy. Ann Neurol. 2005; 58:525–532. [PubMed: 16037972]
37. Lee Y, Messing A, Su M, et al. GFAP promoter elements required for region-specific and astrocyte-specific expression. Glia. 2008; 56:481–493. [PubMed: 18240313]
38. Li T, Lan JQ, Fredholm BB, et al. Adenosine dysfunction in astrogliosis: cause for seizure generation? Neuron Glia Biology. 2007; 3:353–366. [PubMed: 18634566]
39. Li T, Lytle N, Lan J-Q, et al. Local disruption of glial adenosine homeostasis in mice associates with focal electrographic seizures: a first step in epileptogenesis? Glia. 2012; 60:83–95. [PubMed: 21964979]
40. Li T, Ren G, Lusardi T, et al. Adenosine kinase is a target for the prediction and prevention of epileptogenesis in mice. J Clin Inv. 2008; 118:571–582.
41. Li T, Steinbeck JA, Lusardi T, et al. Suppression of kindling epileptogenesis by adenosine releasing stem cell-derived brain implants. Brain. 2007; 130:1276–1288. [PubMed: 17472985]
42. Martin KA. Microcircuits in visual cortex. Curr Opin Neurobiol. 2002; 12:418–425. [PubMed: 12139990]
43. Masino SA, Li T, Theofilas P, et al. A ketogenic diet suppresses seizures in mice through adenosine A1 receptors. J Clin Inv. 2011; 121:2679–2683.
44. Michel CM, Murray MM, Lantz G, et al. EEG source imaging. Clin Neurophysiol. 2004; 115:2195–2222. [PubMed: 15351361]
45. Najm IM, Tilelli CQ, Oghlakian R. Pathophysiological mechanisms of focal cortical dysplasia: a critical review of human tissue studies and animal models. Epilepsia. 2007; 48 (Suppl 2):21–32. [PubMed: 17571350]
46. Neirinckx RD. Evaluation of regional cerebral blood flow with 99mTc-d, 1 HM-PAO and SPECT. Neurosurg Rev. 1987; 10:181–184. [PubMed: 3332036]
47. O'Regan ME, Brown JK. Abnormalities in cardiac and respiratory function observed during seizures in childhood. Dev Med Child Neurol. 2005; 47:4–9. [PubMed: 15686283]
48. Oghlakian RO, Tilelli CQ, Hiremath GK, et al. Single injection of a low dose of pentylenetetrazole leads to epileptogenesis in an animal model of cortical dysplasia. Epilepsia. 2009; 50:801–810. [PubMed: 19396951]
49. Pelligrino DA, Vetri F, Xu HL. Purinergic mechanisms in gliovascular coupling. Semin Cell Dev Biol. 2011; 22:229–236. [PubMed: 21329762]
50. Phillis JW. Adenosine and adenine nucleotides as regulators of cerebral blood flow: roles of acidosis, cell swelling, and KATP channels. Crit Rev Neurobiol. 2004; 16:237–270. [PubMed: 15862108]
51. Phillis JW, Lungu CL, Barbu DE, et al. Adenosine's role in hypercapnia-evoked cerebral vasodilation in the rat. Neurosci Lett. 2004; 365:6–9. [PubMed: 15234462]
52. Pignataro G, Maysami S, Studer FE, et al. Downregulation of hippocampal adenosine kinase after focal ischemia as potential endogenous neuroprotective mechanism. J Cereb Blood Flow Metab. 2008; 28:17–23. [PubMed: 17457365]
53. Reif R, Qin J, An L, et al. Quantifying optical microangiography images obtained from a spectral domain optical coherence tomography system. Int J Biomed Imaging. 2012; 2012:509783. [PubMed: 22792084]
54. Schuele SU, Luders HO. Intractable epilepsy: management and therapeutic alternatives. Lancet Neurol. 2008; 7:514–524. [PubMed: 18485315]
55. Schwartz TH, Chen LM, Friedman RM, et al. Intraoperative optical imaging of human face cortical topography: a case study. Neuroreport. 2004; 15:1527–1531. [PubMed: 15194889]
56. Sciotti VM, Van Wylen DG. Increases in interstitial adenosine and cerebral blood flow with inhibition of adenosine kinase and adenosine deaminase. J Cereb Blood Flow Metab. 1993; 13:201–207. [PubMed: 8436611]

57. Shen HY, Lusardi TA, Williams-Karnesky RL, et al. Adenosine kinase determines the degree of brain injury after ischemic stroke in mice. J Cereb Blood Flow Metab. 2011; 31:1648–1659. [PubMed: 21427729]
58. Siegel AM, Jobst BC, Thadani VM, et al. Medically intractable, localization-related epilepsy with normal MRI: presurgical evaluation and surgical outcome in 43 patients. Epilepsia. 2001; 42:883–888. [PubMed: 11488888]
59. Studer FE, Fedele DE, Marowsky A, et al. Shift of adenosine kinase expression from neurons to astrocytes during postnatal development suggests dual functionality of the enzyme. Neuroscience. 2006; 142:125–137. [PubMed: 16859834]
60. Theofilas P, Brar S, Stewart K-A, et al. Adenosine kinase as a target for therapeutic antisense strategies in epilepsy. Epilepsia. 2011; 52:589–601. [PubMed: 21275977]
61. Wang RK. Three-dimensional optical micro-angiography maps directional blood perfusion deep within microcirculation tissue beds in vivo. Phys Med Biol. 2007; 52:N531–537. [PubMed: 18029974]
62. Wang RK, Hurst S. Mapping of cerebro-vascular blood perfusion in mice with skin and skull intact by Optical Micro-AngioGraphy at 1.3 mum wavelength. Opt Express. 2007; 15:11402–11412. [PubMed: 19547498]
63. Wang RK, Jacques SL, Ma Z, et al. Three dimensional optical angiography. Opt Express. 2007; 15:4083–4097. [PubMed: 19532651]
64. Weinberg MS, McCown TJ. Current prospects and challenges for epilepsy gene therapy. Exp Neurol. 2013; 244:27–35. [PubMed: 22008258]
65. Weinberg MS, Samulski RJ, McCown TJ. Adeno-associated virus (AAV) gene therapy for neurological disease. Neuropharmacology. 2013; 69:82–88. [PubMed: 22465202]
66. Wykes RC, Heeroma JH, Mantoan L, et al. Optogenetic and potassium channel gene therapy in a rodent model of focal neocortical epilepsy. Sci Transl Med. 2012; 4:161ra152.

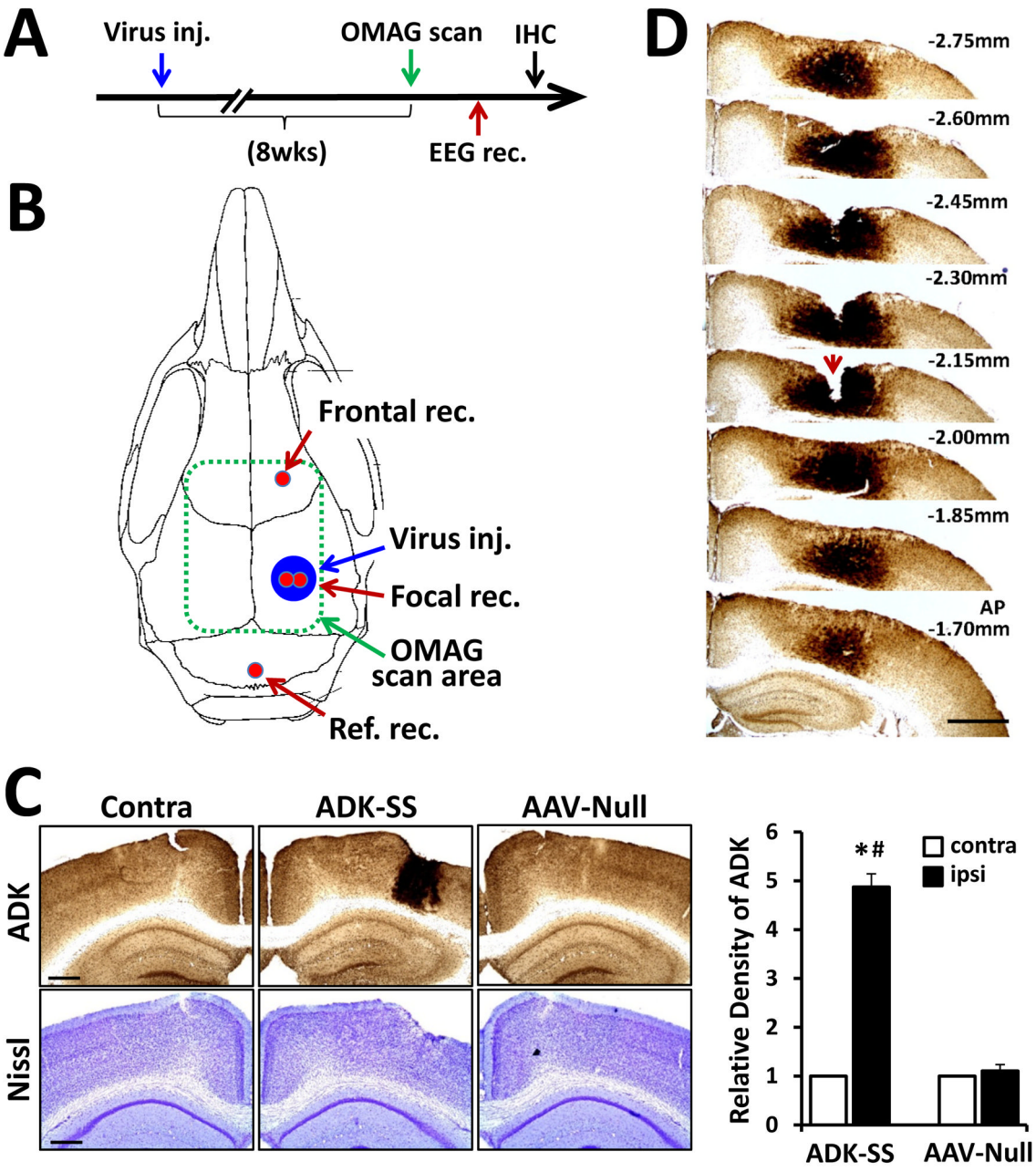

Fig. 1.

Overexpression of ADK in the neocortex of mice induced by unilateral injection of ADK sense (ADK-SS) virus. A: Schematic illustration of the experimental paradigm. Mice were first subjected to unilateral intracortical virus injection, followed after 8 weeks by an OMAG scan and cortical EEG recordings. After completion of the EEG, animals were sacrificed for immunohistochemistry analysis. **B:** Schematic illustration of the virus transduced area (Virus inj.) locations of the EEG recording electrodes (*red*): in frontal cortex (Frontal rec.), focal area of ADK overexpression (Focal rec.), and above the cerebellum (Ref. rec.). The area scanned by OMAG is indicated by a *dashed green line*. **C:** Representative ADK immunoperoxidase (upper panel) and Nissl (lower panel) staining of brain slices showing the contralateral (Contra) or ipsilateral injected (ADK-SS) hemisphere of an ADK-SS

recipient and the virus-injected hemisphere of an AAV-Null injected control animal (AAV-Null). The bar graph demonstrates relative densities of ADK immunoreactivity of DAB-stained brain sections of ADK-SS or AAV-Null virus-injected mice (two sections per animal, n=5 animals per group), scale bar = 500 μm**. D:** Representative ADK staining of consecutive brain slices from an ADK-SS virus-injected animal showing the three dimensional extent of ADK overexpression. Notch (arrow) on −2.15 mm slice indicates the locus of the electrode implantation, scale bar = 1 mm. Data are displayed as mean ± SEM. # P<0.01 ADK-SS *vs* AAV-Null group; * P<0.01 ipsilateral *vs* contralateral side. Abbreviations: Virus inj. = virus injection area; Ref. rec= reference electrode recording; Frontal rec = frontal electrode recording; Focal rec. = electrode recording; contra = contralateral; ipsi = ipsilateral; IHC = immunohistochemistry

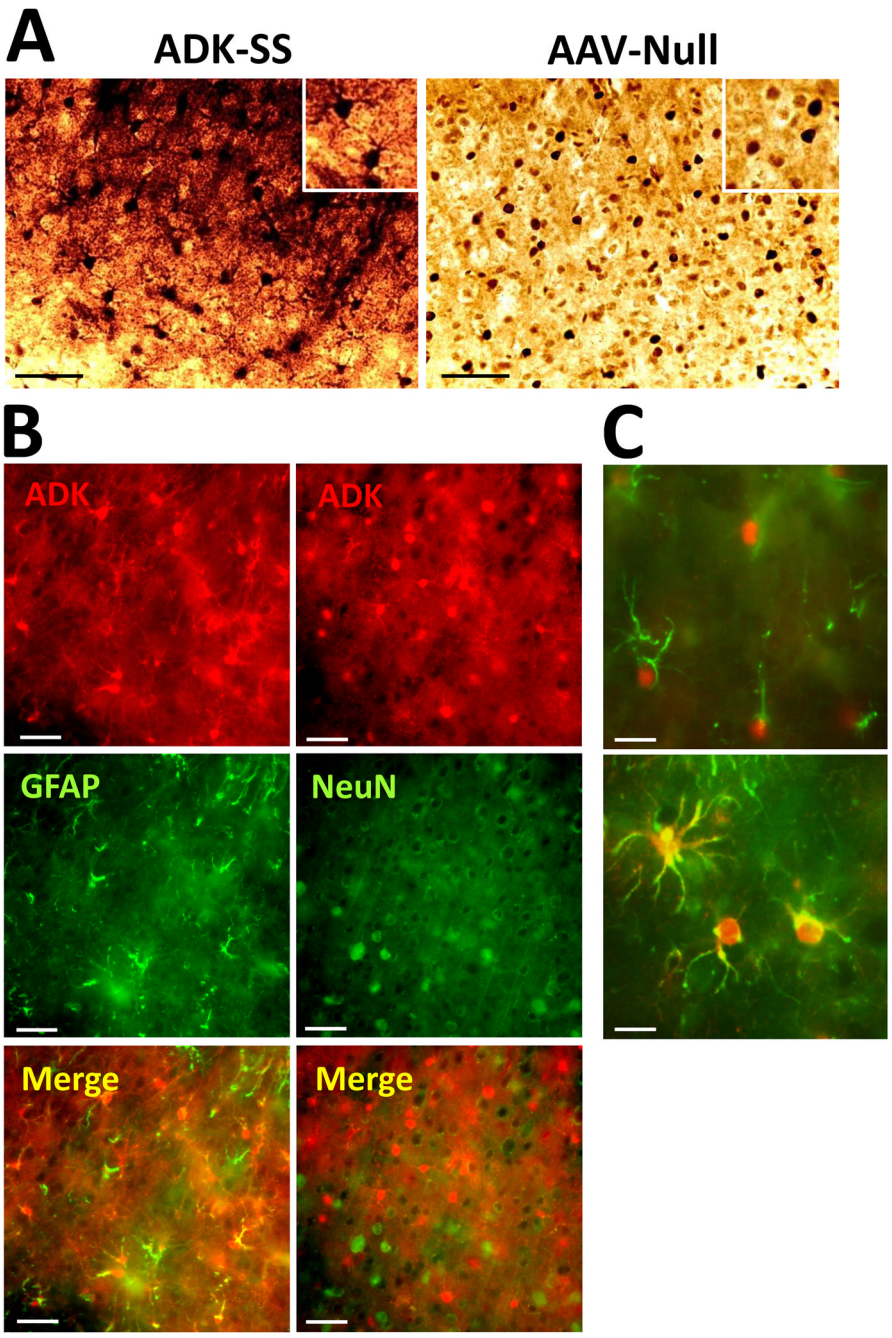

Fig. 2.

Cellular expression pattern of ADK. **A:** ADK immunohistochemistry on coronal sections from mouse brain injected with ADK-SS virus or AAV-Null virus, scale bar = 25 μm. **B:** Immunofluorescence of ADK-SS virus-induced ADK expression (*red*) co-stained with antibodies directed against GFAP, (*green*, left panel) or NeuN (*green*, right panel), scale bar = 25 μm. **C:** Double-immunofluorescence staining of ADK (*red*) and GFAP (*green*) at higher resolution showing expression of endogenous ADK within the nucleus and cell soma of astrocytes from the neocortex of an AAV-Null injected control animal (top) and

expression of exogenous ADK throughout the soma and processes of astrocytes from an ADK-SS recipient, scale bar = 10 μm.

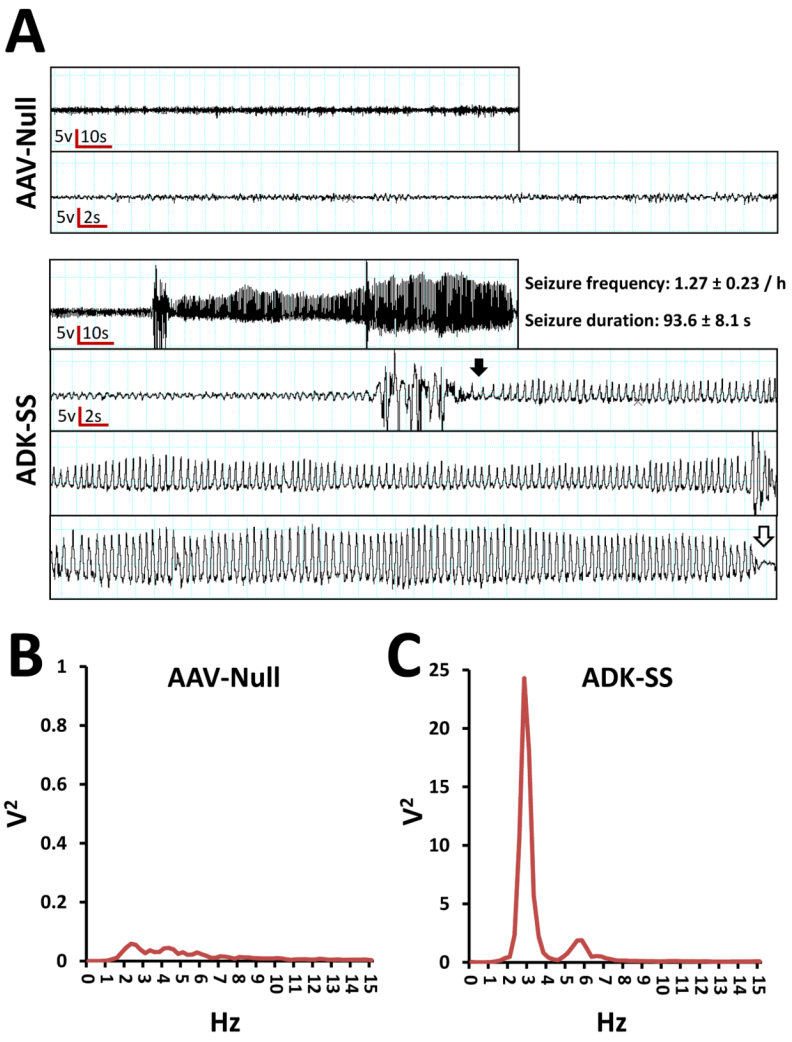

Fig. 3.

Neocortical electroencephalographic activity of AAV-injected mice. **A:** Focal intracortical EEG traces from the neocortical region of mice injected with AAV-Null (upper panel) or ADK-SS (lower panel). The lower traces are at higher resolution and represent background activity (AAV-Null) and a complete representative seizure (ADK-SS) including seizure onset (closed arrow) and end (open arrow). Power spectral analysis of EEG activity from mice injected with **B:** AAV-Null or **C**: ADK-SS.

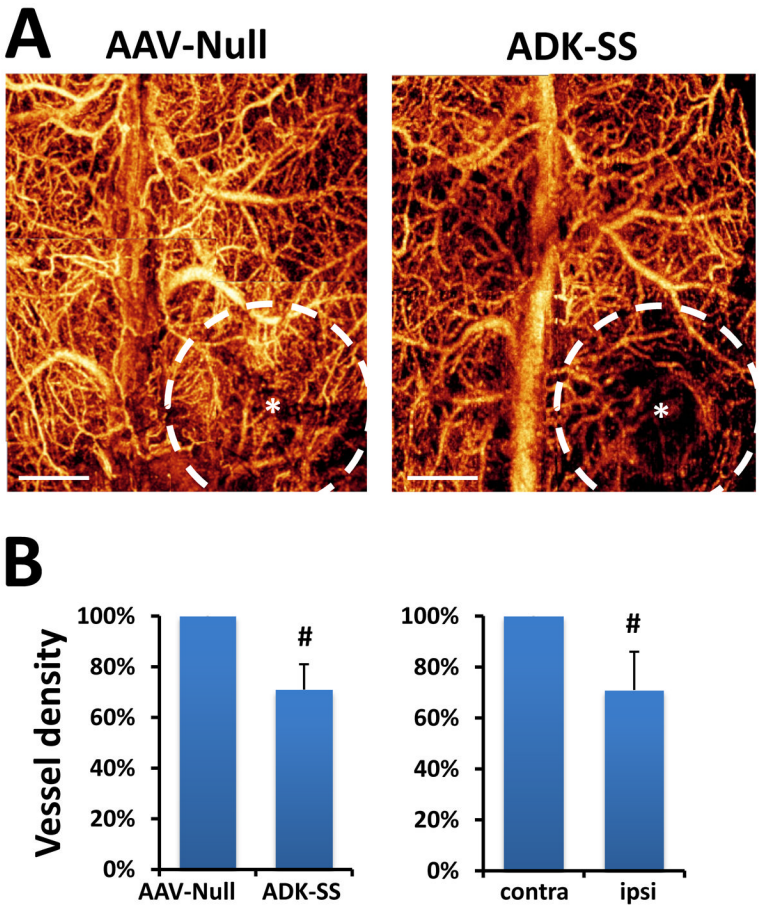

Fig. 4.

OMAG of cerebral blood perfusion and vessel densities in AAV-injected mice. **A:** Representative 2D plane images of cortical vessel density at capillary level resolution in AAV-Null or ADK-SS virus recipients. *indicates the coordinate of virus injection whereas the dashed line indicates the virus-affected area, scale bar = 1 mm. **B:** Quantitative analysis showing reduced cortical vessel density in the hemispheres injected with ADK-SS, compared to those injected with AAV-Null (left panel), or compared to those in the contralateral hemisphere (right panel). Cortical vessel densities are shown as percentage relative to control. Data are displayed as mean ± SEM. # $P<0.05$ paired comparisons t-test (n=5 per group).